A switchable and stable single-longitudinal-mode, dual-wavelength erbium-doped fiber laser assisted by Rayleigh backscattering in tapered fiber

Gu, Jian; Yang, Yanfu; Liu, Meng; Zhang, Jianyu; Wang, Xiaorui; Yuan, Yijun; Yao, Yong

2015

Gu, J., Yang, Y., Liu, M., Zhang, J., Wang, X., Yuan, Y., et al. (2015). A switchable and stable single-longitudinal-mode, dual-wavelength erbium-doped fiber laser assisted by Rayleigh backscattering in tapered fiber. Journal of Applied Physics, 118(10), 103107-.

https://hdl.handle.net/10356/79326

https://doi.org/10.1063/1.4930054

AIP Journal of Applied Physics

A switchable and stable single-longitudinal-mode, dual-wavelength erbium-doped fiber laser assisted by Rayleigh backscattering in tapered fiber

Jian Gu, Yanfu Yang, Meng Liu, Jianyu Zhang, Xiaorui Wang, Yijun Yuan, and Yong Yao

Citation: Journal of Applied Physics **118**, 103107 (2015); doi: 10.1063/1.4930054
View online: http://dx.doi.org/10.1063/1.4930054
View Table of Contents: http://scitation.aip.org/content/aip/journal/jap/118/10?ver=pdfcov
Published by the AIP Publishing

A switchable and stable single-longitudinal-mode, dual-wavelength erbium-doped fiber laser assisted by Rayleigh backscattering in tapered fiber

Jian Gu,[1] Yanfu Yang,[1,a)] Meng Liu,[2] Jianyu Zhang,[1] Xiaorui Wang,[1] Yijun Yuan,[1] and Yong Yao[1]
[1]*College of Electronic and Information Engineering, Shenzhen Graduate School, Harbin Institute of Technology, Shenzhen, Guangdong Province 518055, China*
[2]*School of Electrical and Electronic Engineering, Nanyang Technological University, 50 Nanyang Avenue, Singapore, 639798 Singapore*

(Received 14 May 2015; accepted 23 August 2015; published online 10 September 2015)

We have proposed and demonstrated a novel switchable single-longitudinal-mode (SLM), dual-wavelength erbium-doped fiber laser (DWEDFL) assisted by Rayleigh backscattering (RBS) in a tapered fiber in a ring laser configuration. The RBS feedback in a tapered fiber is a key mechanism as linewidth narrowing for laser output. A compound laser cavity ensured that the EDFL operated in the SLM state and a saturable absorber (SA) is employed to form a gain grating for both filtering and improving wavelength stability. The fiber laser can output dual wavelengths simultaneously or operate at single wavelength in a switchable manner. Experiment results show that with the proper SA, the peak power drift was improved from 1–2 dB to 0.31 dB and the optical signal to noise ratio was higher than 60 dB. Under the assistance of RBS feedback, the laser linewidths are compressed by around three times and the Lorentzian 3 dB linewidths of 445 Hz and 425 Hz are obtained at 1550 nm and 1554 nm, respectively. © *2015 AIP Publishing LLC*.
[http://dx.doi.org/10.1063/1.4930054]

I. INTRODUCTION

Single-longitudinal-mode (SLM), Dual-wavelength erbium-doped fiber lasers (DWEDFL) have attracted much attention and have wide applications in optical fiber sensing,[1] fiber communications,[2] biomedicine,[3] material processing,[4] and wavelength division multiplexing (WDM)[5] because of their advantages such as high output power, high tuning efficiency, outstanding beam quality, and long working life. Several techniques for obtaining dual-wavelength operations have been proposed, including Brillouin scattering, phase-shift Bragg grating, linear overlapping cavity, cascaded Sagnac loop interferometer, passively Q-switched loop cavity with grapheme and single-wall nanotube saturable absorber, dual-loop cavity, and actively Q-switched linear cavity.[6–13] Because dual-wavelength ring fiber lasers usually have long cavity,[7] many longitudinal modes can exist around the lasing center wavelength. To achieve a stable SLM operation in the EDFL, two kinds of cavities can be carefully adopted. One is a short length cavity, which consequently increases longitudinal mode spacing.[14] However, the lasers may suffer from low slope efficiency. The other one is long length ring cavity to offer higher output power. Meanwhile, an ultra-narrow band-pass filter must be used to eliminate multi-longitudinal-mode (MLM) oscillation and mode hopping.[15] To achieve SLM operation, various mode suppression techniques have been proposed, such as phase-shifted fiber Bragg grating (FBG) with ultra-narrow bandwidth,[16] a high finesse FBG based Fabry-Perot (FP) etalon,[17] a compound ring,[17,18] passive multiple ring cavities,[18,19] a saturable absorber (SA) inducing spatial-hole burning as a dynamic narrow bandwidth filter[20] and a FBG as self-injection feedback.[21,22] Combining these controlling technologies with FBG, intra-cavity FP filter or FBG based FP etalon,[17] both wavelength tunable and SLM operation have been realized simultaneously.[17,18]

In this paper, we demonstrated a novel switchable SLM, DWEDFL assisted by Rayleigh backscattering (RBS) in a tapered fiber in a ring laser configuration. It is well known that electrostriction is the dominant effect to generate stimulated Rayleigh scattering (STRS) and the gain coefficient of stimulated Brillouin scattering (SBS) is two orders of magnitude higher than that of STRS in single mode fiber, so the special optical fiber with high SBS threshold should be used to suppress SBS in order to collect STRS. In this work, we have fabricated a standard single-mode-fiber (SMF) fiber (∼150 m) with ∼30 tapers to suppress SBS. As a result, the collected STRS effect in the tapered fiber has a key role for linewidth narrowing. Meanwhile, a SA with optimized length and a compound-cavity configuration are employed together in the laser cavity to achieve stable SLM operation. Finally, the fiber laser can work in dual-wavelength mode or in switchable single wavelength between two.

II. EXPERIMENTAL SETUP AND PRINCIPLE

A. Fabrication and characterization of the tapered fiber

In optical fiber, the electrostriction is the dominant effect to generate STRS. Because the gain coefficient of SBS in

a)yangyanfu@hotmail.com

standard SMF is normally two orders of magnitude higher than that of STRS,[23,24] STRS is buried by SBS. With the precondition that SBS is suppressed, STRS can be excited under high pump power. In view of physics principle, Brillouin scattering in optical fiber is a fundamental interaction between light (photons) and phonons (acoustic waves), as shown in the Fig. 1. It has been verified experimentally that photonic crystal fibers (PCFs) with novel micro/nanostructure allows for a tight confinement of both photons and phonons, leading to new characteristics for Brillouin scattering different from those of standard optical fibers.[25] Hence, we employed a simple tapered fiber fabricated by a flame brush method. Similar to PCFs, the tapered fiber has varied shape and core size in order to modify the interaction effect between photons and phonons. From Ref. 26, we know that SBS occurs in optical fiber when two counter propagating optical waves have a precise frequency offset called phonons Brillouin frequency shift (BFS), $v_B = 2n_{eff}V_a/\lambda$,[27] where λ is the optical wavelength in vacuum, n_{eff} is the effective refractive index of the fiber, and V_a is the acoustic velocity. Both n_{eff} and V_a are determined by the fiber materials and optical/acoustic waveguide structure. Chung *et al.*[28] proved that BFS continuously increases according to the decrease of the taper diameter. The Brillouin gain g_B can be expressed as $g_B = (4\pi n_{eff}^8 P_{12}^2)/(c\rho\lambda^3 v_B \triangle v_B)$,[27] where P_{12}^2 is the elasto-optic constant, ρ is the mean density of fused silica, c is the speed of light in vacuum, λ is the optical wavelength and $\triangle v_B$ is the Brillouin linewidth ($\sim$20 MHz). The SBS threshold has the following standard formula: $P_{th} = (21A_{eff})/(Kg_B L_{eff})$,[27] where A_{eff} is the effective area, L_{eff} is the effective length that accounts for losses, and the K is the polarization factor. It can be found in the formula that P_{th} is proportional to the BFS.

Figure 1 shows the schematic illustration of one taper fiber. Our fabricated tapered fiber has the length of around 150 m with 30 tapers. Each taper has the length l of $\sim$3 cm and has taper diameter around 70 μm. In the tapered fiber, the SBS threshold is measured to be larger than that in single mode fiber by around 6 dB. This means that the better collection of STRS effect can be obtained via our fabricated tapered fiber under larger scattering coefficient and SBS threshold.

B. SLM operation principle

As we all know that free spectral range (FSR) is inversely proportional to the cavity length according to the principle of ring cavity laser as

$$FSR = \frac{c}{nL}, \tag{1}$$

where L is the total cavity length, n is the effective refractive index of the fiber which is assumed as 1.46, and c is the speed of light in vacuum. In this experimental setup, the main cavity length is $\sim$320 m, the FSR_{Main} is $\sim$642 kHz, and according to Eq. (1), the small FSR makes it hard to achieve SLM operation. Here, the compound cavity is employed to increase FSR. As shown in the dashed box in Fig. 2, a 10 m compound cavity is made using 3 dB coupler (C_1) with the resultant $FSR_{compound}$ of 20 MHz. Based on the Vernier effect, the equivalent FSR of the laser cavity is huge, which should be the least common multiple of FSR_{main} and $FSR_{compound}$. Thus, the MLM oscillation is suppressed to ensure the SLM operation of the EDFL.

As shown in Fig. 2, the main cavity is incorporated with two optical FBGs (FBG_1 and FBG_2) having the reflective wavelengths of 1550 nm and 1554 nm. Two FBGs has the maximum reflectivity of about 90% and the 3 dB bandwidth of around 0.3 nm. An unpumped EDF_2 with proper length is inserted as an SA between OC_1 and FBG_2 to achieve single-mode selection. When light from OC_1 port 2 meets the reflected light from two FBGs, the interference results in standing waves in the SA and consequently generate a periodic intensity distribution. The caused gain saturation and index modulation in the unpumped EDF_2 actually forms self-induced FBG, which has the function of mode filtering and frequency stabilizing. The reflective bandwidth of self-induced FBG[27] can be expressed by

$$\Delta f = \frac{c}{\lambda}\frac{2\Delta n}{n_{eff}\lambda}\sqrt{\left(\frac{\Delta n}{2n_{eff}}\right)^2 + \left(\frac{\lambda}{2n_{eff}L_g}\right)^2}, \tag{2}$$

where λ is the center wavelength of the self-induced FBG, n_{eff} is the effective refractive index of the SA, c is the speed of

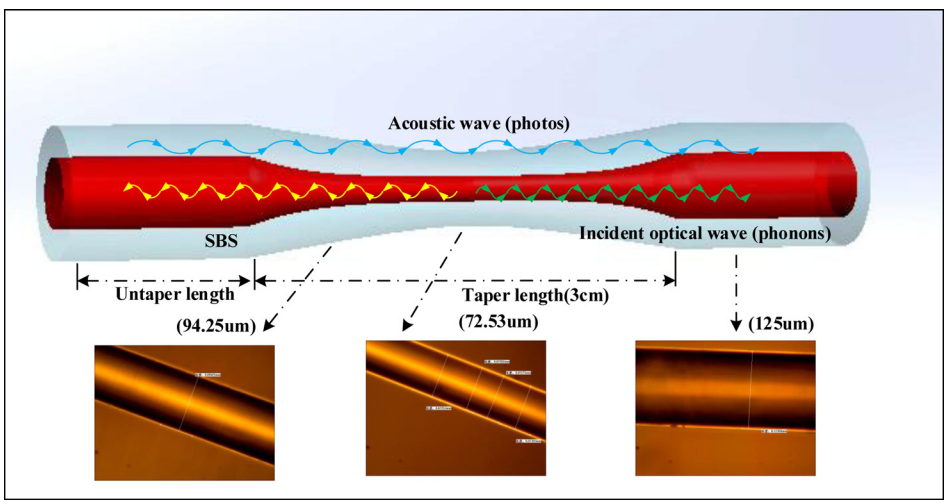

FIG. 1. Schematic diagram of one optical fiber taper and the SBS effect between incident light (photons) and phonons (acoustic waves).

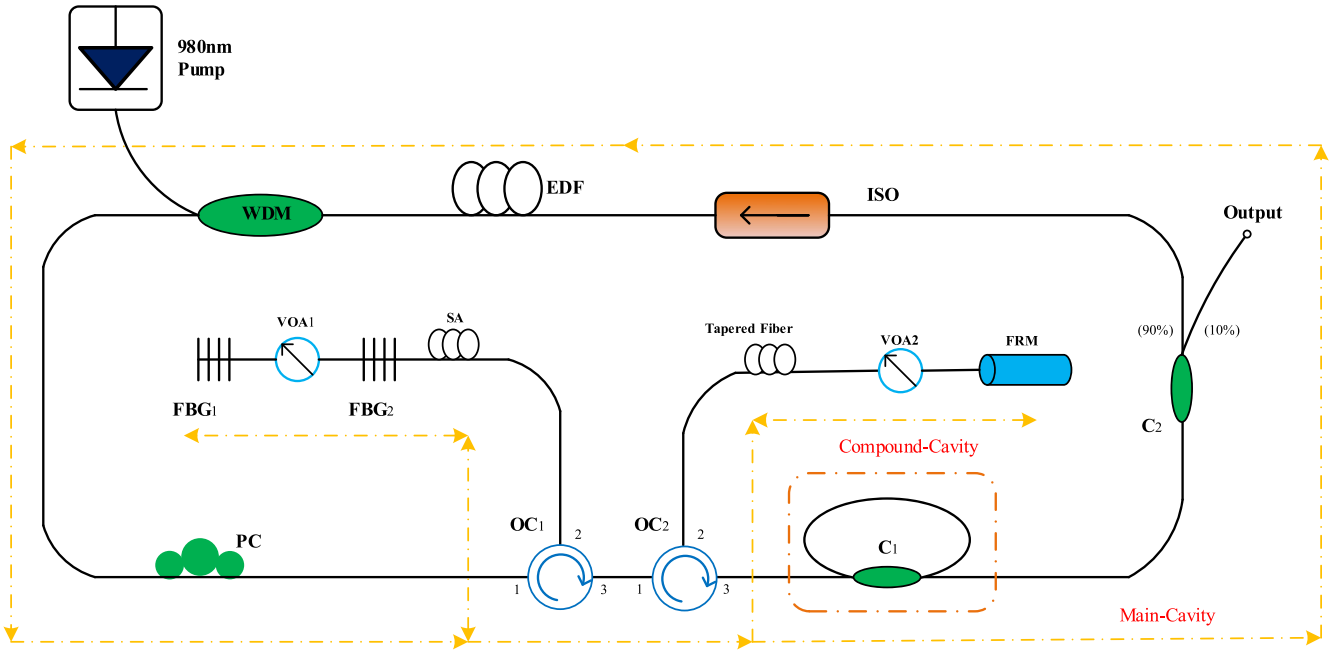

FIG. 2. Experimental setup of the proposed switchable dual-wavelength SLM-EDFL.

light in vacuum, L_g is the SA length, and Δn is the induced refractive index change in SA. With the parameters of $\lambda = 1550$ nm or 1554 nm, $n_{eff} = 1.46$, $L_g = 3$ m, $\Delta n = 1.5 \times 10^{-7}$, the full width at half maximum (FWHM) (Δf) of the self-induced FBG is estimated to be ~8.5 MHz from Eq. (2).

III. EXPERIMENTS AND DISCUSSION

The experimental setup of our proposed switchable and stable SLM, dual-wavelength EDFL is mainly consisted of a saturable absorber, a compound cavity, and a tapered fiber, as shown in Fig. 2. In the main cavity, a 10 m EDF is pumped by a 980 nm pump laser. Two FBGs serve as a lasing wavelength selector. The variable optical attenuator (VOA_1) is used to adjust the loss of the cavity in order to configure single- or dual-wavelength lasing. The isolator can be used to avoid the SA being pumped by the 980 nm laser. The light from port 2 of OC_2 is launched into the tapered fiber that is used to generate STRS light, and then is reflected by a Faraday rotation mirror (FRM) to form a standard ring laser. The distributed STRS light in the tapered fiber is coupled back to the cavity through port 3 of OC_2. Here we need a VOA_2 to adjust the cavity loss and suppress side modes, in which the STRS can be the main scattering light in the tapered fiber. This configuration is critical in seeding an STRS source to compress the linewidth.

First, the influence of the SA length on the output laser spectrum is investigated and the role of SA for improving lasing stability is confirmed. In our fiber ring laser shown in Fig. 2, one FBG with the center wavelength of 1549.5 nm and our fabricated tapered fiber are employed. The VOA_2 is removed to ensure that the reflected pump signal is dominant and the STRS signal can be negligible. As a result, the fiber laser becomes a traditional ring fiber. The measured optical spectrum of the laser output under different pump laser ranging from 55 mW to 300 mW are plotted in Figs. 3(a)–3(c) for different length SA. With 1 m SA, there exist obvious spurs at side lope of the measured optical spectrum. This can be attributed to the degraded bandwidth and extinction ratio in the resultant transmission profile by self-induced FBG in short unpumped SA. In the case of the longer SA of 6 m, the laser spectrum becomes unstable. This can be understood considering the large absorption and the resultant cavity loss for the longer SA. With the moderate SA of 3 m used, the spectrum quality and the wavelength stability can be improved significantly. The linewidth of the output laser at 1549.5 nm is measured using delayed self-heterodyne detection (DSHM) method. An acoustic optic modulator (AOM) with a frequency shift ~80 MHz is used, and a 50 km SMF-28 fiber is used as the delay-line. The linewidth of the ring laser signal can be measured by the electrical spectrum analyzer (ESA), as shown in Fig. 3(d). In order to increase the measurement accuracy, the 20 dB linewidth is estimated to be 24.4 kHz based on the fitting curve of the measured electrical spectrum. The Lorentzian 3 dB linewidth can be calculated as 1/20 of the 20 dB linewidth and is equal to around 1.22 kHz.

Fig. 4 presents the measured spectrum of the laser output with the resolution bandwidth of 0.1 nm when the VOA_1 is adjusted continuously. In the cavity, the loss of each wavelength can be changed by turning VOA_1. Because of the existence of gain competition, usually a wavelength oscillates and the other one is suppressed. However, when the cavity loss at the two wavelengths is equal, the competition is reduced and dual-wavelength output can be achieved. As a consequence, VOA_1 have been placed between two FBGs in order to correctly adjust the cavity losses on each wavelength to achieve oscillation of the system at the desired wavelengths. With the adjustment of VOA_1, the difference of the cavity loss between 1550 nm and 1554 nm are varied correspondingly. When the pump is increased to 108 mW, our

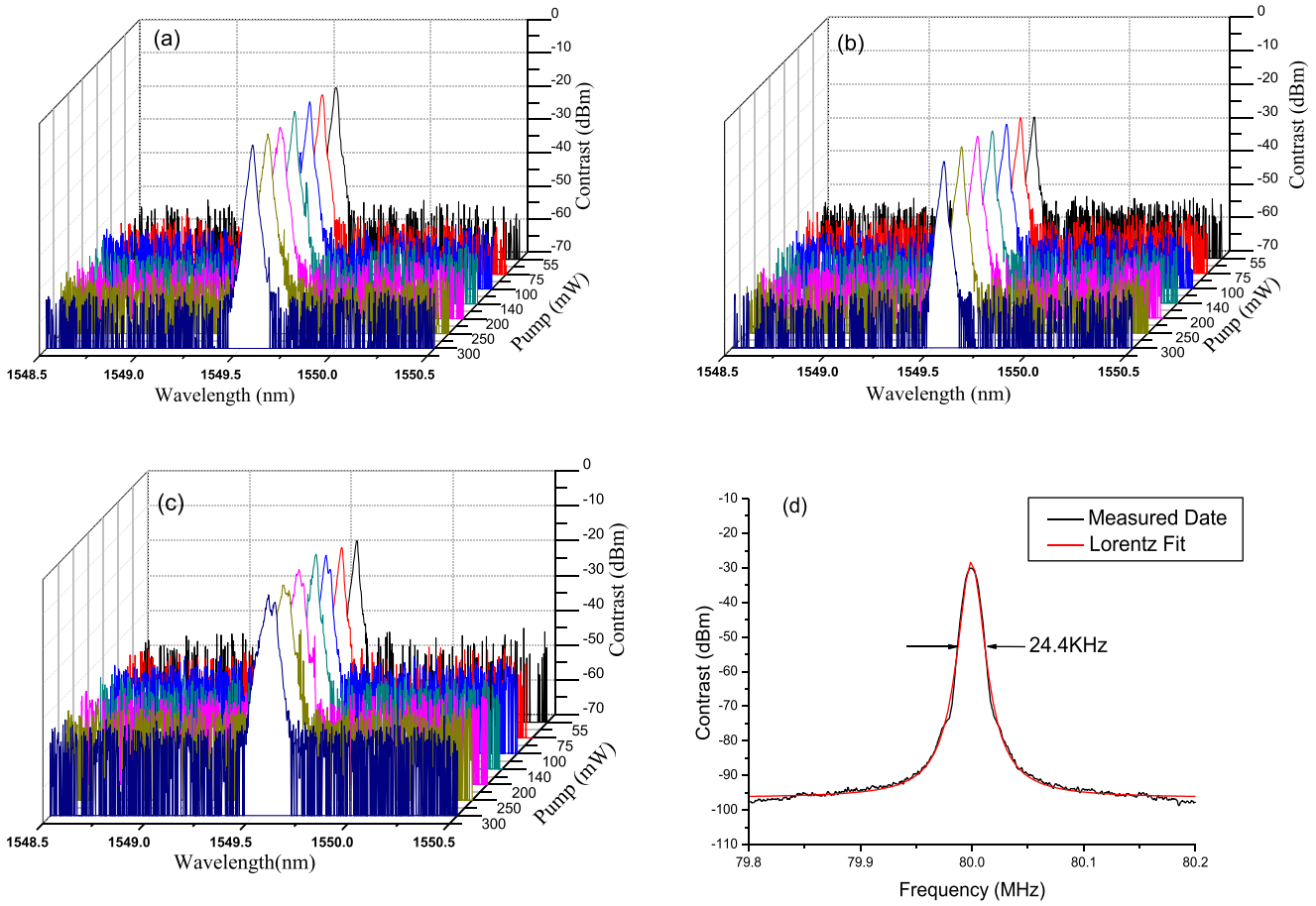

FIG. 3. The measured optical spectrum of single wavelength laser at 1549.5 nm with different length SA employed: (a) 1 m, (b) 3 m, (c) 6 m, and (d) the measured linewidth results with 3 m SA.

proposed EDFL can work in a switchable manner or in dual wavelength mode successfully. The obtained optical signal to noise ratio (OSNR) is higher than 60 dB. Besides, the power stability function of the SA in the proposed EDFL has also been proved experimentally. As shown in Fig. 5, with 3 m SA, the power variation for the laser outputs at 1550 nm and 1554 nm has been reduced from more than 2 dB to less than 0.5 dB.

In the following, the linewidth compression role of the STRS feedback in a tapered fiber in the proposed switchable SLM, dual-wavelength EDFL will be confirmed. The VOA_2 is inserted to the cavity, and two FBGs with two wavelengths ($\lambda_1 = 1550$ nm and $\lambda_2 = 1554$ nm) can be used. Meanwhile, the 3 m SA is employed to improve the spectrum quality and the wavelength stability as above. In the experiment, VOA_2 with proper attenuation is set to suppress the reflected pump light from the FRM. The Rayleigh scattering occurs at multiple scattering centers along the tapered fiber. VOA_2 can be used to suppress the reflected pump light contribution to the EDF gain, so the Rayleigh backscattering signal is collected

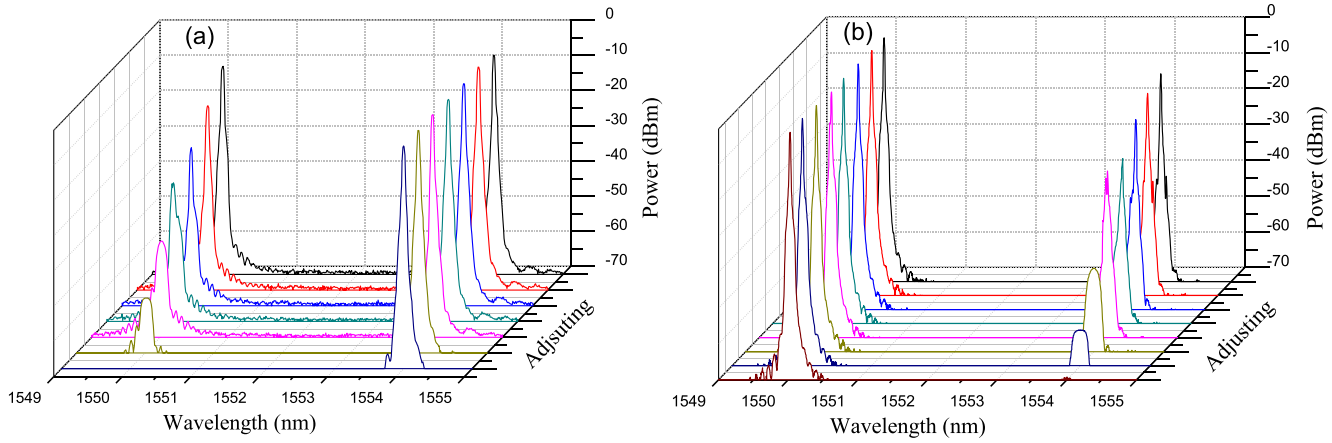

FIG. 4. The measured optical spectrum of the fiber laser with the adjustment of VOA_1.

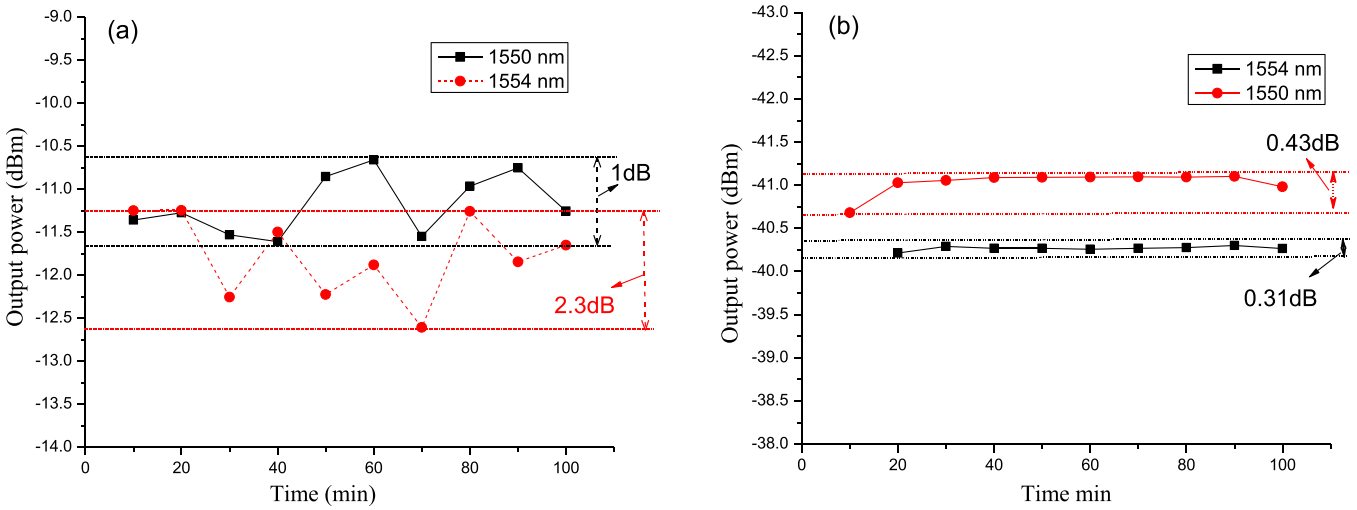

FIG. 5. The power stability of the laser at 1550 nm and 1554 nm: (a) without 3 m SA and (b) with 3 m SA.

effectively and will not be buried by the reflected light. Consequently, a distributed mirror is formed and lead to the diffusion of effective cavity length. Therefore, the STRS can play a role of linewidth compression.[24] The linewidth and single-longitudinal mode performance of the lasing output in single-wavelength operation at λ_1 (1550 nm) and λ_2 (1554 nm) are characterized by using DSHM. The measured spectrums and the Lorentz fitting curves are indicated by the solid lines and dashed lines, respectively. As shown in Fig. 6, the 20 dB linewidths from the peaks in the fitting curves are 8.9 kHz and 8.5 kHz, respectively. Based on the relationship that the Lorentzian 3 dB linewidth of laser is equal to be

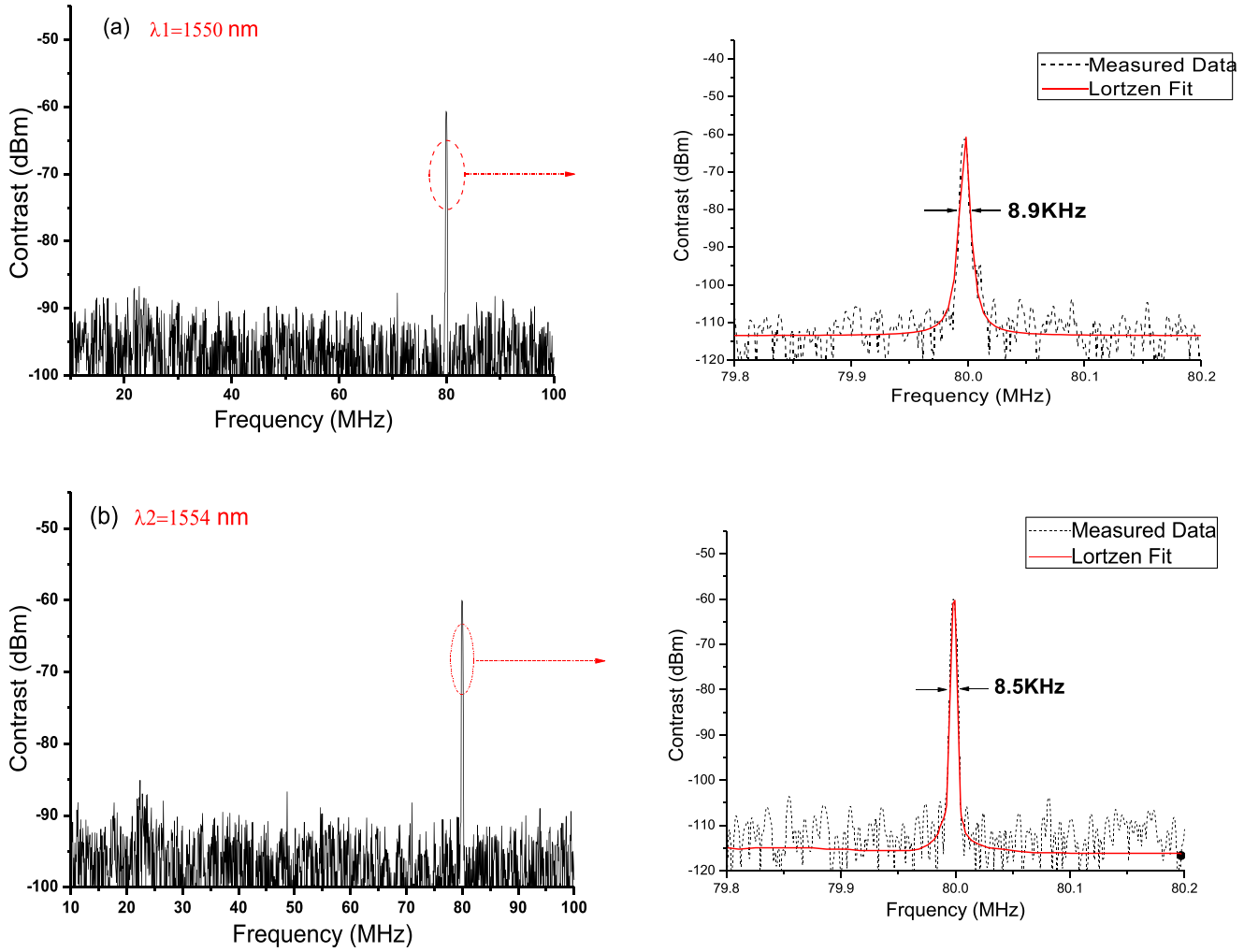

FIG. 6. The linewidth measurement in dual-wavelength operation: (a) 1550 nm and (b) 1554 nm.

1/20 of 20 dB linewidth, the EDFL lasing at $\lambda 1$ and $\lambda 2$ has the 3 dB linewidth of about 445 Hz and 425 Hz, respectively. Compared to the linewidth result in Fig. 3(d), the compression of around three times is achieved with the help of the distributed STRS effect.

IV. CONCLUSION

We successfully demonstrated a novel switchable SLM, DWEDFL assisted by Rayleigh backscattering in a tapered fiber in a ring laser configuration. The round-trip and amplifying RBS feedback in fiber laser is a key to compress the linewidth of the laser output. The compound-cavity ensured the EDFL operated in the SLM state and a SA is employed to form a gain grating for both filtering and improving the laser stability. Experiment results illustrate that the peak power drift is less than 0.5 dB, and the signal to noise ratio was higher than 60 dB. With the simple adjustment of VOA, the fiber laser can work in a switchable manner or in two wavelength lasing output simultaneously. The 3 dB linewidths at two wavelengths are measured to be approximately 445 Hz and 425 Hz.

ACKNOWLEDGMENTS

This work was supported by the National Natural Science Foundation of China (Contract No. 61205046) and Shenzhen Municipal Science and Technology Plan Project (JCYJ20150327155705357).

[1]Z. R. Lin, C. K. Liu, and G. Keiser, Optik **123**(1), 46–48 (2012).
[2]V. Mizrahi, D. J. DiGiovanni, R. M. Atkins, S. G. Grubb, Y. K. Park, and J. M. Delavaux, J. Lightwave Technol. **11**(12), 2021–2025 (1993).
[3]H. Y. Meng, J. H. Liao, and B. G. Guan, Chin. J. Lasers **34**(5), 733–736 (2007).
[4]H. B. Tang, X. Li, D. Liu, and S. Q. Zhang, Chin. J. Lasers **1**, 021 (2012).
[5]C. A. Brackett, IEEE J. Sel. Areas Commun. **8**(6), 948–964 (1990).
[6]Y. Yao, X. Chen, Y. Dai, and X. Z. Xie, IEEE Photonics Technol. Lett. **18**(1), 187–189 (2006).
[7]A. E. El-Taher, M. Alcon-Camas, S. A. Babin, P. Harper, J. D. Ania-Castañón, and S. K. Turitsyn, Opt. Lett. **35**(7), 1100–1102 (2010).
[8]Q. H. Mao and J. W. Y. Lit, IEEE Photonics Technol. Lett. **14**(9), 1252–1254 (2002).
[9]D. S. Moon, G. Sun, and A. Lin, Opt. Commun. **281**(9), 2513–2516 (2008).
[10]H. Ahmad, A. A. Latif, and M. I. M. Abdul Khudus, Appl. Opt. **52**(4), 818–823 (2013).
[11]X. Zhao, Z. Zheng, L. Liu, Y. Liu, Y. X. Jiang, and X. Yang, Opt. Express **19**(2), 1168–1173 (2011).
[12]M. A. Ummy, N. Madamopoulos, P. Lama, and R. Dorsinville, Opt. Express **17**(17), 14495–14501 (2009).
[13]M. Durán-Sánchez, E. A. Kuzin, O. Pottiez, A. González-Garcíaand, and B. Ibarra-Escamilla, Laser Phys. Lett. **11**(1), 015102 (2014).
[14]X. He, X. Fang, and C. Liao, Opt. Express **17**(24), 21773–21781 (2009).
[15]G. Yin, B. Saxena, and X. Y. Bao, Opt. Express **19**(27), 25981–25989 (2011).
[16]X. Chen, J. Yao, and F. Zeng, IEEE Photonics Technol. Lett. **17**(7), 1390–1392 (2005).
[17]X. P. Cheng, P. Shum, and C. H. Tse, IEEE Photonics Technol. Lett. **20**(12), 976–978 (2008).
[18]T. Feng, F. Yan, and S. Liu, Laser Phys. Lett. **11**(12), 125106 (2014).
[19]T. Feng, F. Yan, and S. Liu, Laser Phys. **24**(8), 085101 (2014).
[20]T. Liao, J. Zhao, and C. Zhang, Laser Phys. **24**(1), 015104 (2014).
[21]J. Zhao, C. Zhang, and C. Miao, Opt. Commun. **331**, 229–234 (2014).
[22]L. Zhu, W. He, and Y. Zhang, Opt. Fiber Technol. **20**(5), 487–490 (2014).
[23]T. Zhu, X. Y. Bao, and L. Chen, Opt. Express **18**(22), 22958–22963 (2010).
[24]T. Zhu, X. Y. Bao, and L. Chen, J. Lightwave Technol. **29**(12), 1802–1807 (2011).
[25]J. E. McElhenny, R. K. Pattnaik, and J. Toulouse, J. Opt. Soc. Amm. B **25**(4), 582–593 (2008).
[26]A. Kobyakov, M. Sauer, and D. Chowdhury, Adv. Opt. Photonics **2**(1), 1–59 (2010).
[27]J. C. Beugnot, Nat. Commun. **5**, 5242 (2014).
[28]K. H. Chung, S. B. Lee, and K. Y. Song, in *OptoElectronics and Communication Conference and Australian Conference on Optical Fiber Technology* (2014), pp. 1039–1040.